Absence of giant dielectric permittivity in graphene oxide materials Absence of giant dielectric permittivity in graphene oxide materials

M Alfonso, Jinkai Yuan, F Tardani, W Neri, A Colin, P Poulin

Absence of giant dielectric permittivity in graphene oxide materials

JPhys Materials

PAPER

Absence of giant dielectric permittivity in graphene oxide materials

M Alfonso[1], J Yuan[1], F Tardani[1], W Neri[1], A Colin[1,2] and P Poulin[1]

[1] Univ. Bordeaux, CNRS, Centre de Recherche Paul Pascal, UMR5031, 33600 Pessac, France
[2] CBI-MIE, ESPCI Paris, 10 Rue Vauquelin, Paris F-75005, France

E-mail: philippe.poulin@crpp.cnrs.fr

Keywords: graphene oxide, dielectric, permittivity, capacitor

Supplementary material for this article is available online

OPEN ACCESS

RECEIVED
5 March 2019

REVISED
14 May 2019

ACCEPTED FOR PUBLICATION
3 June 2019

PUBLISHED
22 July 2019

Abstract

Graphene oxide (GO) is considered as a promising component for electronics because of its unique anisotropy, easy processing and sometimes claimed giant permittivity. The latter would arise from an enhanced electronic polarizability due to the presence of functional groups at the surface and edge of GO flakes. As a matter of fact, a number of publications have reported a very large permittivity of GO materials. Nevertheless, the reported values for the intrinsic relative permittivity vary significantly from a few units to several millions. Such variability raises a critical question on the actual and intrinsic permittivity of GO, and on difficulties of measurements due to the polarization of the electrodes. We presently report impedance spectroscopy characterizations of GO solutions with different solvents. We find very large capacitance at low frequencies, in agreement with previous reports. However, we also show that these results can be interpreted without considering a giant permittivity of GO. Actually, a simple equivalent circuit model allows us to confirm that GO does not have a giant permittivity. We conclude that GO can be used as an electrolyte for supercapacitors, or as a precursor for electrically conductive graphene-based materials, but not as an efficient additive to raise the permittivity of solvents or composites for electronics and energy storage applications.

Introduction

Graphene oxide (GO) is an oxidized form of graphene [1, 2]. It is generally obtained by acid treatment of graphitic materials. By contrast to graphene, GO is insulating due to heavy functionalization with oxygen groups, and to the subsequent disruption of the conjugated network of sp^2 carbon atoms. Nevertheless, GO displays particularly appealing features as such. It is soluble in polar solvents, including water, and can be easily processed into films and fibers [3–5].

It has a high flexibility along with a high Young's modulus [6]. In addition, it can be used as a precursor for graphene based materials since electronic conjugation and conductivity can be partially restored after reduction [1, 2].

GO is also often considered as a promising material for electronics and energy storage applications in which high-permittivity materials are sought after. Actually, according to various studies, GO materials could even display a giant permittivity with values which vary in a wide range and usually greater than 10^3.

For example, Liu *et al* [7] reported that GO can be used as a high-k material for energy storage applications with a dielectric constant greater than 1000 at 100 Hz. Hong *et al* drew the same conclusion [8] and Huang *et al* [9] reported values of relative permittivity above 100 at 100 Hz. Kumar *et al* have reported even greater values, up to 10^6 at 1 kHz [10].

As stated by the authors, these giant dielectric constants would arise from the orientational polarization of oxygen-containing groups at the surface of GO planes and along the edges [10, 11]. Very large permittivities have also been reported for GO based foams and sensors in absence of humidity [11–14]. According to the authors, the capacitive behavior of GO paper for sensing shows a strong dependence on temperature and relative humidity. A strong increase of relative permittivity by around 3 orders of magnitude occurs with decreasing humidity with capacitance values from several hundreds of pF to several hundreds of nF [15].

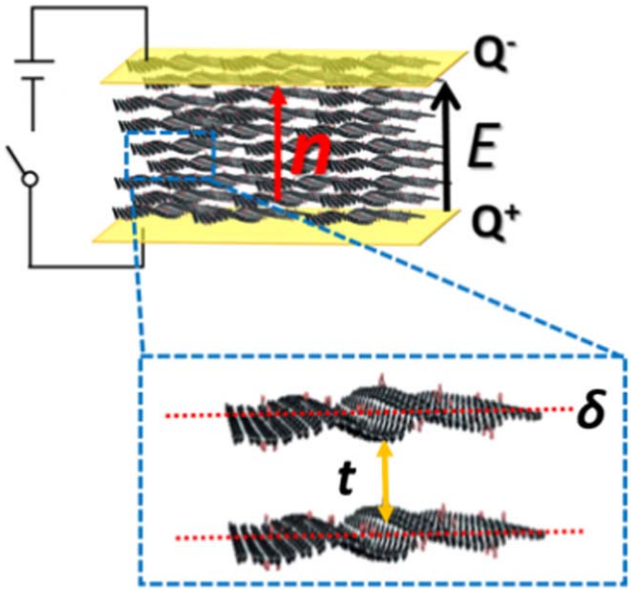

Figure 1. Schematic representation of GO dispersion in a pseudo-lamellar phase with the normal of the particles parallel to the direction of the electric field and with δ the thickness of the stacked dielectric insulating GO layers and t the thickness of the separating solvent layers.

Large values of relative dielectric permittivity are also suggested from characterizations of composite materials in which a small fraction of GO added to a polymer enhances the effective permittivity of the composite [16–22]. By contrast, other studies have reported more moderate values of permittivity, of about 3, or less, in frequency ranges typically from 100 to 1000 Hz [23–26]. Uses of GO as dielectrics in transistors led also to the conclusion that GO has a relative permittivity typically between 3 and 5 [27–29].

Enhancements of permittivity are, as for neat GO based materials, deduced from measurements of large capacitances. Nevertheless, the origin of such large dielectric permittivities remains unclear. Al-Zangana *et al* [30] have recently investigated dielectric relaxation processes of GO solutions in isotropic fluids or liquid crystals (LCs). Relaxations in 2-Propanol are associated with very large amplitudes, well above 1000 in relative permittivity at 1 kHz. Such a giant amplitude would reflect a giant intrinsic dielectric constant of GO particles.

One can indeed expect, in the most optimistic case, that the GO dispersions form a pseudo-lamellar phase in the investigated concentration ranges [31, 32].

In this case, the system can be modeled as a heterogeneous medium with stacked insulating GO layers separated from each other by solvent layers as shown in figure 1. Each GO layer has a thickness δ and a complex conductivity $\sigma^*_{GO} = 2\pi j\nu\varepsilon_0\varepsilon_{GO}$ while the solvent layers have a thickness t and a complex conductivity $\sigma^*_{Solv} = \sigma_{Solv} + 2\pi j\nu\varepsilon_0\varepsilon_{Solv}$, where ε_0 is the permittivity of vacuum, ε_{GO} and ε_{solv} the dielectric constants of GO and of the solvent, σ_{solv} the conductivity of the solvent and ν the frequency.

Considering that $t \gg \delta$ and that the normal of the layers is parallel to the electric field, in order to predict the greatest possible permittivity, the effective complex permittivity of the solution ε_{eff} is given by $\varepsilon^*_{eff} = \frac{\Delta\varepsilon}{1+j\frac{\nu}{\nu_0}} + \varepsilon_{Solv}$ with $\Delta\varepsilon = \varepsilon_{GO}\frac{t}{\delta}$ and $\nu_0 = \frac{\delta\sigma_{Solv}}{2\pi\varepsilon_0 t\varepsilon_{GO}}$.

The above assumptions are reasonable considering the actual size of GO particles and the fact that they display thermal undulations of small amplitude [6]. The inclusion of GO in a given fluid is therefore expected to generate a dielectric relaxation with an amplitude that is proportional to its intrinsic dielectric constant. This is why very large amplitudes should reflect a giant dielectric constant of GO. The same actually would hold for various GO polymer composites developed for energy storage applications, and which display very large effective dielectric constants. Nevertheless, we have to keep in mind that the large permittivities reported in the literature are deduced from capacitance measurements in complex electrical circuits. As already discussed by some authors [16–18], other mechanisms, and in particular polarization of electrodes could contribute to the capacitance measurements.

Separating the contribution of electrode polarization (EP) from the volumetric one is often challenging. GO, by contrast to neat graphene or other graphitic particles, can be viewed as a polyelectrolyte, which carries a huge number of counter-ions. The latter, be they in liquids or polymers, can form ionic double layers at the surface of

electrodes and generate a large effective capacitance. Moreover, GO can also adsorb at the electrode interface and contribute to the EP [26].

In order to clarify the situation and determine whether GO displays a giant permittivity or not, we propose in this work a simple approach which consists in measuring the impedance of dielectric cells filled with GO solutions at different concentrations. This approach, called impedance spectroscopy, is broadly used to determine the permittivity and conductivity of materials. We model the system using an equivalent circuit by considering both the contribution of electrodes, for an interfacial capacitance, and that of the dielectric medium, for the volumetric capacitance [33]. We use a dielectric cell designed to enhance the contribution of the bulk compared to that of the electrode surface. The present cell is made of platinum rectangular electrodes and has a very low constant cell.

As previously observed in the literature, experiments both in Milli-Q water and in 2-Propanol confirm the measurements of very large capacitance at low frequencies. However, our simple modeling also demonstrates that the observed capacitances can be simply explained by polarization of electrodes, without considering neither giant permittivity of GO nor specific relaxation modes related to the rotation of the particles [30]. We therefore conclude that GO is not a high-permittivity material potentially useful for energy storage applications. However, it remains a unique precursor, easily processable, to make graphene-based materials, after reduction [1, 2].

Indeed, as already well established, reduced GO is a conducting material. As such, it can enhance the permittivity of composites at concentrations in near-percolated regimes [34–40].

Experimental section

Materials

Commercial GO solution in water with a concentration of 4 mg ml^{-1} was purchased from Graphenea (Spain). This dispersion is prepared by chemically processing raw graphite material in water via the modified Hummer's method [41]. According to the provider, the monolayer content, measured with 0.05 wt% dispersion, reaches values up to 95% and the single layer has a sheet dimension of 5–7 μm (see figures S1 and S2 in the supplementary information available online at stacks.iop.org/JPMATER/2/045002/mmedia). Note that because of polydispersity, particles greater than 7 μm or smaller than 5 μm can be found in the samples. The degree of oxidation is around 40% as measured by x-ray photoelectron spectroscopy (XPS) analysis (figure S3). The oxidized functions include approximately C–OH 284 eV, C=O 288 eV, O=C–OH 291 eV [42]. Milli-Q water (Q-Gard 00D2) with a resistivity above 18.2 MΩ cm at 25 °C and 2-Propanol (IPA) absolute 99.9% were purchased from Sigma Aldrich and used as received.

Sample preparation

The GO dispersions in Milli-Q water and IPA were obtained through a solvent exchange process. First, aqueous GO solution was centrifuged at 50 000 g for 1 h (Sorval RC 6+, rotor SE-12). The collected slurry was then dissolved in pure IPA. The obtained diluted dispersions in IPA were then centrifuged at 1400 g for 20 min (Jouan B4i Multifunction, rotor S40) in order to precipitate any large aggregates. The supernatant was collected and treated using the same procedures as above to perform the second and third solvent exchanges. Afterwards, the achieved GO/IPA dispersion was sonicated with a tip Branson Sonifier 450 A for 30 min at 135 W to further improve the dispersion state of GO flakes.

This procedure allows the unbundling of the small remaining aggregates. Note that sonication presumably induces a slight reduction of the size of the flakes [43]. Nevertheless, as shown further, the GO particles remain sufficiently large in diameter to form LC phases at relatively low concentration. The obtained dispersions were then subjected to a final ultracentrifuge process at 50 000 g for 1 h to achieve GO gel with a high concentration of 65 mg ml^{-1}. The concentration was determined by dry extract characterizations of the samples. 1 g of the final gel was dried in a muffle furnace at 90 °C under vacuum for a duration of 2 h. Samples with different weight percentage (wt%) of GO flakes were prepared by dilution in IPA.

The GO dispersions in Milli-Q water were prepared with exactly the same protocols. Note that at high concentration, the GO solutions display a high viscosity and a yield stress [5–44]. The systems are kept at room temperature during the present study. Increase of temperature can induce reduction of the particles, making them hydrophobic and electrically conductive.

Related materials have been characterized by x-ray diffraction in previous studies, and have been shown to be relatively stable against reduction [6, 31]. The pH of the solutions, measured on litmus paper, varies typically between 5 and 6 in the investigated concentration range. There was not a significant effect of pH observed.

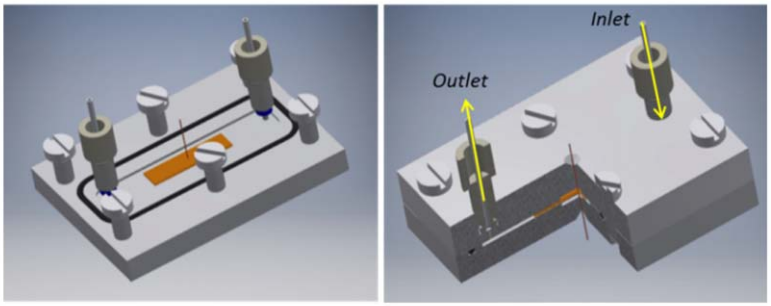

Figure 2. The schematic image of the home-built dielectric cell used in this work. The inlet and outlet present on top of the dielectric cell are necessary for insertion of the sample.

Characterization

Polarizing optical micrographs (Leica DM 2500 P) of GO dispersions in Milli-Q water and IPA were taken to investigate their birefringence at room temperature. The dielectric properties of the obtained dispersions were studied by using an impedance analyzer (7260 Impedance Analyzer, Materials Mates Italia) under a voltage of 50 mV in a frequency range of 100 Hz–10^6 Hz. The measurements were performed using a home-built cell with two platinum electrodes, as shown in figure 2.

The size of the electrodes is 24 mm $\times$ 4 mm and the separation between them is 500 μm. The cell thickness was calibrated by measurements of sodium chloride water solution with difference concentrations with known conductivity (see supplementary information figure S9). The large surface area of the electrodes and the thin thickness were designed to minimize the strong effect of the polarization of the electrodes and maximize the contribution of the bulk [45]. The present cell has a cell constant of only 5.2 $\times$ 10^{-3} mm^{-1}.

Results and discussion

Optical micrographs of GO dispersions in Milli-Q water and IPA are shown in figure 3. GO flakes are homogeneously dispersed at low concentration, with a small number of microscopic aggregates below 0.6 wt% in Milli-Q water and 0.4 wt% in 2-Propanol. Cross-polarizing pictures show increasing birefringence (bright spots) as approaching the biphasic-nematic phase boundary, around 0.8 wt% GO, for both solvents with increasing GO concentration.

In the nematic phase (figures 3 (D), (E) and (I), (J)), no aggregation is detected. Note that the presence or absence of aggregates is more clearly evaluated using unpolarized light (figures 3 (A′)–(J′)) compared to images using crossed polarizers (figures 3(A)–(J)). The flakes alignment is increasing, as evidenced by the increasing size of birefringent domains.

Due to the large size dispersity, no clear lamellar phase is observed, as expected for plate-like nanoparticles systems.

Nevertheless, the formed nematic phase can be viewed as a pseudo-lamellar phase with a regular spacing between the flakes [6, 31]. The present phase behavior is consistent with that observed in previous reports [31, 46–48] and was not investigated in more depth in the present work.

GO LCs contain a rather large amount of ionic species which affect the determination of their dielectric properties due to a strong interfacial polarization, also called EP. GO contains indeed a large fraction of functional groups such as carboxylic groups and dissociated counter ions. The polar solvents contain protons and hydroxyl ions.

They can also contain ions due to the dissolution of CO_2. The EP is due to the adsorption of ions and formation of a diffuse double layer [45] at the metal/solution interface. This phenomenon induces a large capacitive behavior at low frequencies, when the electric field inversion is slow enough so that the motion of ionic charges is hindered by the charging of the electric double layer. By contrast, at high frequencies the polarity inversion is fast enough to keep the charge carriers moving.

For a quantitative analysis of the system and in order to differentiate the electric double layer capacitance from the dielectric behavior of the bulk, one can use an effective equivalent electrical circuit (EEC) model [33, 49] (see supplementary information figure S5). Because no particular ionic or electronic relaxation is expected at a molecular scale on the frequency range of investigation, we consider the circuit elements as

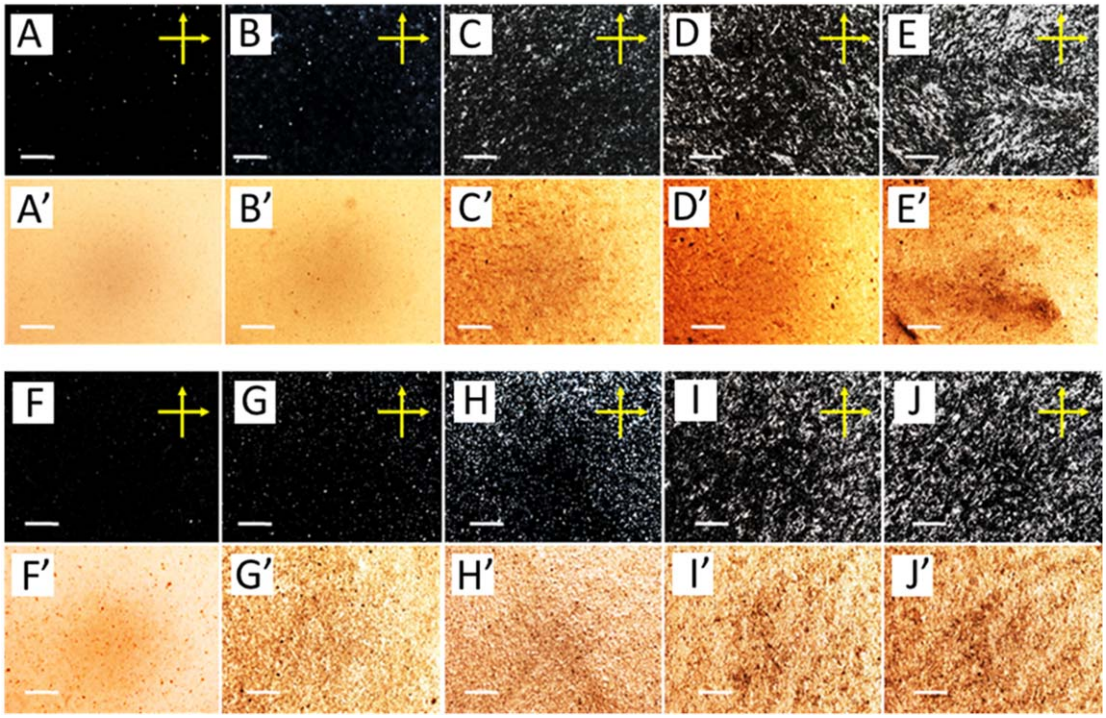

Figure 3. Optical polarizing micrographs of GO dispersion in Milli-Q water (A)–(E) and 2-Propanol (F)–(L): (A), (F) 0.4 wt%, (B), (G) 0.6 wt%, (C), (H) 1.0 wt%, (D), (I) 1.5 wt%, (E), (J) 3.0 wt%. (Scale bar 200 μm). The observed textures reflect the formation of small monodomains of nematic LC phase.

constant. Several models for GO-based LCs have been reported in the literature. They vary in complexity but were found in most cases suitable to explain experimental measurements in a certain frequency range [50].

First of all, it is necessary to ensure that the volumetric capacitance of the bulk sample is sufficiently large so that it can be measured by the experimental instrumentation. This is why we presently use a cell with a very low constant cell (5.2×10^{-3} mm^{-1}), taking into account that the smallest capacitance accurately measurable with our instrument is on the order of one pF, a common value for commercially available impedance analyzers.

We perform measurements between 100 Hz and 1 MHz, also a typical frequency range use in impedance spectroscopy. It is preferable that relaxation modes fall in this frequency range in order to achieve more accurate fitting of experimental data.

Herein, we adopted a simple EEC model that physically represents the mechanisms involved in the charge storage and transport of the material. This model is an extension of the classical Randles cell model [33, 51, 52].

The found values of capacitances exceed well 10 pF and are associated, for most of them, to relaxations clearly observed between 100 Hz and 1 MHz. In details, this simple model comprises a finite diffusion Warburg element W [53] to account for the diffusion of charged species through the LC. This element is in series with a resistor R_p to model the resistance associated to the polarization of the electrodes.

Both of them are in parallel with a capacitor C_{dl} to take into account the possible accumulation of charges at the interface for an adsorbed double layer capacitance. The capacitor C_{bulk}, represents the volumetric capacitance of the bulk dispersions. This capacitance is directly linked to the permittivity of the sample, whereas the resistor R_s is the resistance of the bulk dispersion due to the ionic species in solution.

The theoretical impedances were calculated based on the EEC model. The impedances associated to the circuit elements are given in figure S5. Such EEC model gives us a satisfying fitting from 100 Hz to 1 MHz. However, this model is not able at describing the properties at frequencies well below 100 Hz, or well above 1 MHz, due to the crude assumption of considering the impedance of each circuit element independent on frequency. In particular, the strong and dominant polarization of electrodes at low frequencies is expected to display a more complex behavior. Calculated values are then compared with the experimental data.

Figure 4 shows the frequency dependence of the real and imaginary parts of the impedance for GO dispersions in 2-Propanol and Milli-Q water. It is observed that impedances are larger for IPA than for Milli-Q water. This is due to the greater permittivity of water compared to IPA, and to the greater ionic conductivity in water. The experimental impedances of samples at different GO concentrations matched well with the

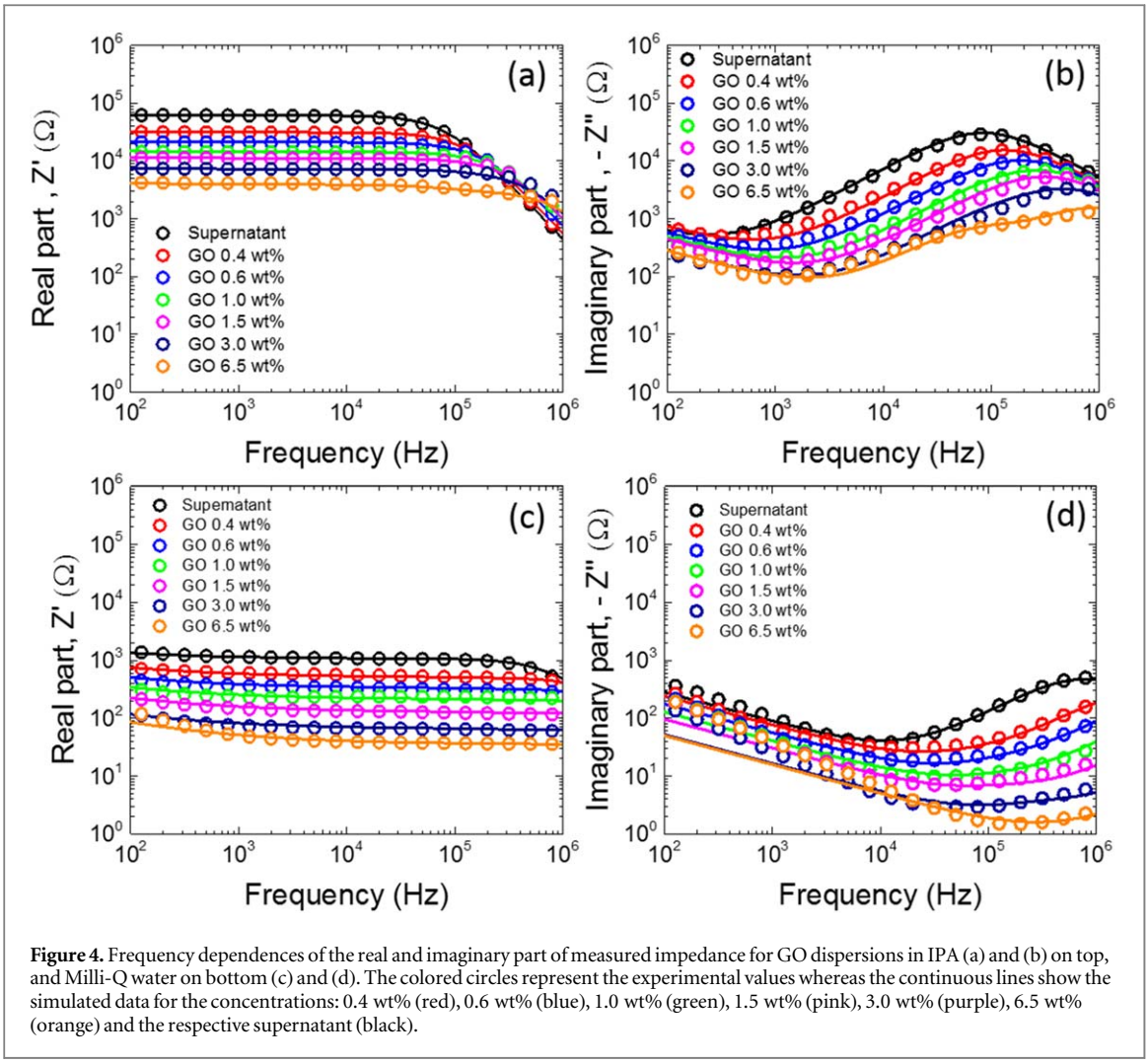

Figure 4. Frequency dependences of the real and imaginary part of measured impedance for GO dispersions in IPA (a) and (b) on top, and Milli-Q water on bottom (c) and (d). The colored circles represent the experimental values whereas the continuous lines show the simulated data for the concentrations: 0.4 wt% (red), 0.6 wt% (blue), 1.0 wt% (green), 1.5 wt% (pink), 3.0 wt% (purple), 6.5 wt% (orange) and the respective supernatant (black).

theoretical curves (colored circles represent the experimental values whereas the continuous line represents the calculated ones). This agreement suggests that the proposed electrical circuit model is suitable and accurate enough to well describe the electrical behavior of our systems. We also stress that the fits are accurate enough to determine the volumetric capacitance. As shown in supplementary information (figure S6), slight changes of the volumetric capacitance lead to poor fitting. The real part of the impedance for dispersions in 2-Propanol, as can be seen in figure 4(a), decreases by an order of magnitude with increasing concentration of GO.

This trend reflects how the resistance R_s of the samples decreases with increasing the GO flake concentration. The imaginary part of the impedance, shown in figure 4(b), also decreases as the concentration of the GO flakes increases, showing a maximum peak starting from 10 kHz, which reflects a capacitive mode behavior. These peaks shift to high frequency with increasing GO concentration.

Concerning the GO dispersions in Milli-Q water, the behaviors of the real and imaginary parts of the impedance are slightly different. This can be attributed to the higher polarity and permittivity of the solvent, which lead to relaxation modes slightly above 1 MHz.

The real part of the impedance, shown in figure 4(c), decreases with the GO concentration. This result reflects again a decrease of resistance of the bulk, which confirms that GO acts as a simple electrolyte in solution. In addition, the real part of the impedance in Milli-Q water shows a relaxation at frequency above 1 MHz, in agreement with other studies [54].

Nevertheless, the lack of full relaxation in the investigated range of frequencies makes the fitting with our model slightly more difficult. In parallel, the maximum of the imaginary part of the impedance, showed in figure 4(d) is not completely visible in the investigated frequency range. The values of each element of the EEC model for the best fitting are given in table 1.

Figure 5 shows the trends of the bulk resistance, R_s, and the related conductivity σ for GO dispersions in 2-Propanol (a) and Milli-Q water (c), calculated through the following expression:

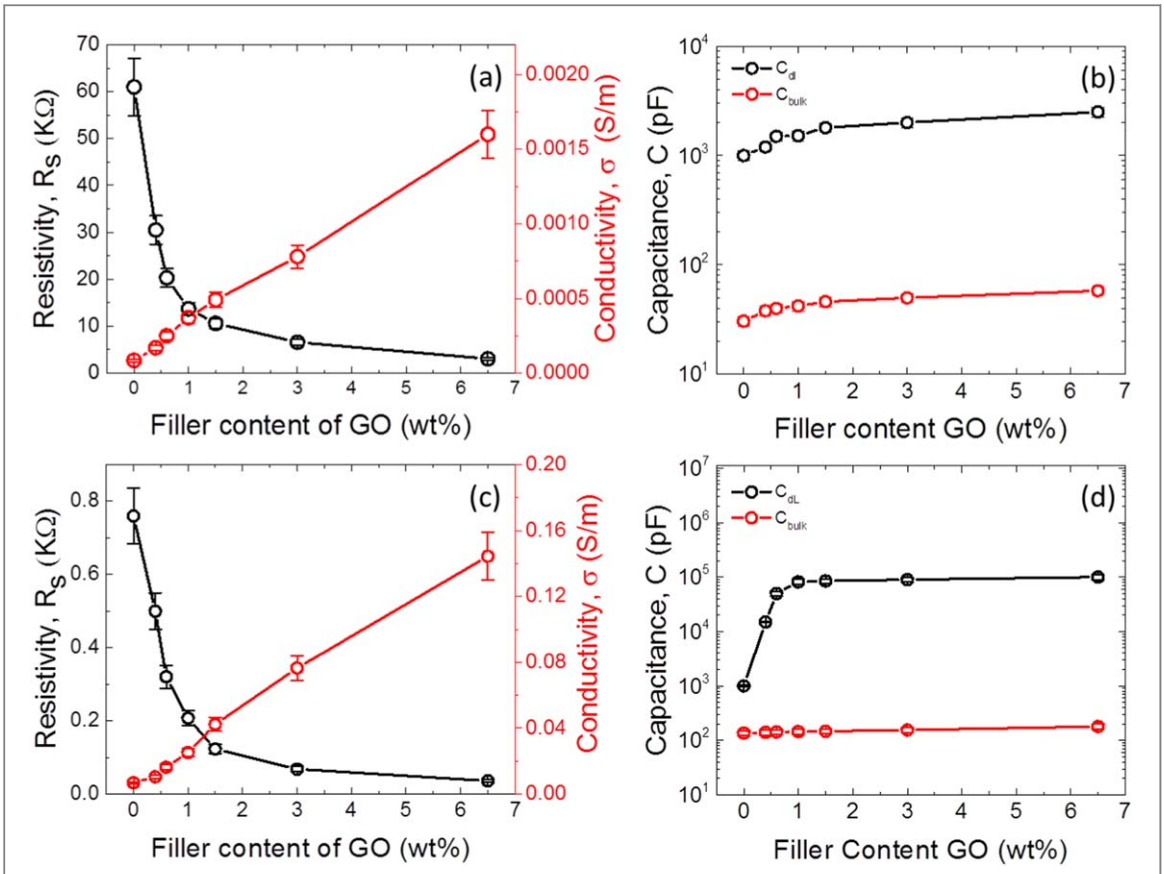

Figure 5. Resistance of the bulk dispersions, R_s and capacitance values of C_{dL} and C_{bulk} as function of weight fraction for GO dispersions in IPA (a), (b) and Milli-Q water (c), (d).

Table 1. The values of each element of the equivalent electrical circuit model (EEC) obtained from data fitting.

Solvent	GO [wt%]	R_p [Ω]	W [Ω]$^{-0.5}$	C_{dl} [F]	R_s [Ω]	C_{bulk} [F]
2-Propanol	Supernatant	800	14 000	1.00×10^{-9}	61 000	3.05×10^{-11}
	0.4 wt%	700	18 000	1.20×10^{-9}	30 500	3.80×10^{-11}
	0.6 wt%	800	14 000	1.50×10^{-9}	20 300	4.00×10^{-11}
	1.0 wt%	700	12 000	1.52×10^{-9}	13 700	4.20×10^{-11}
	1.5 wt%	500	11 000	1.80×10^{-9}	10 600	4.60×10^{-11}
	3.0 wt%	600	7000	2.00×10^{-9}	6600	5.00×10^{-11}
	6.5 wt%	800	7000	2.50×10^{-9}	3070	5.80×10^{-11}
Mili-Q water	Supernatant	300	7000	1.00×10^{-9}	760	1.36×10^{-10}
	0.4 wt%	20	6000	1.50×10^{-8}	500	1.40×10^{-10}
	0.6 wt%	15	4400	5.00×10^{-8}	320	1.43×10^{-10}
	1.0 wt%	9	3200	8.20×10^{-8}	207	1.45×10^{-10}
	1.5 wt%	7	2400	8.50×10^{-8}	123	1.47×10^{-10}
	3.0 wt%	4	1300	9.00×10^{-8}	62	1.55×10^{-10}
	6.5 wt%	1	1250	1.00×10^{-7}	36	1.65×10^{-10}

$$\sigma = \frac{d}{R_s A} \tag{1}$$

with, d equal to 500 μm and A equal to 96 mm^2.

The linear increase in conductivity with GO concentration shows that the GO particles behave as a classical electrolyte in solution.

Ionic conductivity values of bulk dispersions are shown in table 2. It is interesting to note that the ionic conductivity of the supernatant is rather large, even greater than that of NaCl solutions (see table S2). This large ionic conductivity comes from the dissociation of chemical functionalities at the surface of the GO particles.

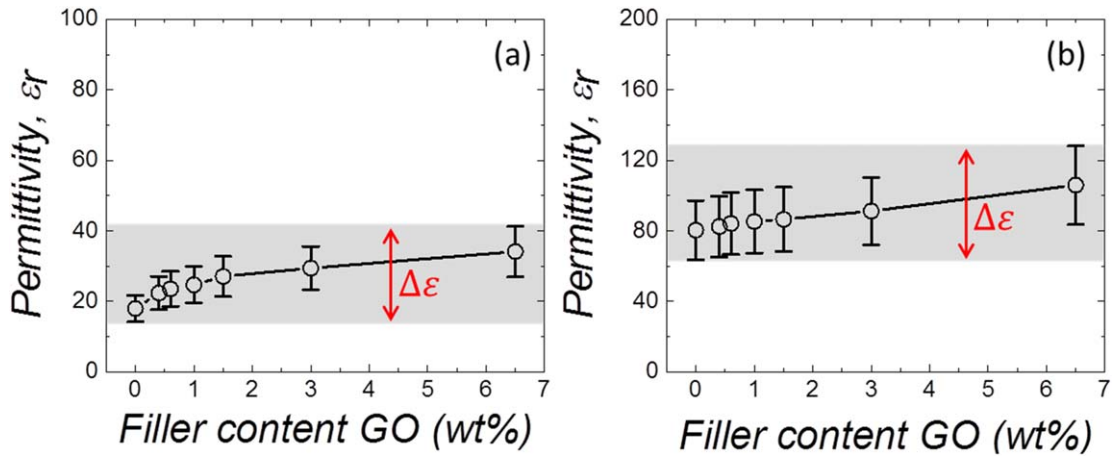

Figure 6. Deduced permittivity of the dispersions as function of concentration for GO dispersions in 2-Propanol (A) and Milli-Q water (B).

Table 2. Ionic conductivity of the bulk dispersions.

		Supernatant	0.4 wt%	0.6 wt%	1.0 wt%	1.5 wt%	3.0 wt%	6.5 wt%
2-Propanol	σ [S m^{-1}]	8.8×10^{-5}	1.7×10^{-4}	2.6×10^{-4}	3.8×10^{-4}	4.9×10^{-4}	7.8×10^{-4}	1.6×10^{-4}
Milli-Q water	σ [S m^{-1}]	6.8×10^{-3}	1.0×10^{-2}	1.6×10^{-2}	2.5×10^{-2}	4.2×10^{-2}	8.4×10^{-2}	1.4×10^{-1}

The fitting of the data also allows the volumetric capacitance of the bulk and the double layer capacitance to be determined. For the dispersions in IPA, the electric double layer capacitance increases from 1 nF, for the supernatant, to 2.5 nF for a concentration of 6.5 wt% of GO.

This increase can be ascribed to the greater concentration of ionic species at the surface of the electrodes. The bulk capacitance evolves from 30 pF for the supernatant, to 58 pF for a concentration of 6.5 wt% of GO.

Regarding GO dispersions in Milli-Q water, the interface capacitance evolves from 1 to 100 nF for a dispersion of 6.5 wt% of GO. The bulk capacitance, increases from 136 pF for the supernatant to 180 pF for the highest GO concentration.

The relative permittivity of the samples can be deduced from the capacitance of the bulk [26] using equation (2):

$$C_{\text{Bulk}} = \varepsilon_0 \varepsilon_r \frac{A}{d}. \tag{2}$$

In figure 6, it is possible to observe how the permittivity of the dispersions grows with the concentration of GO. This increase is clear but not as large as the increase which could have been expected if GO would have had a giant permittivity. As mentioned previously, GO LCs can be considered as a heterogeneous system of planar 2D particles in a pseudo-lamellar phase in which the amplitude $\Delta\varepsilon$ (understood as the difference between the ε_r of GO at 6.5 wt% and the one of the supernatant) is related to the dielectric constant of the particles ε_p as follows:

$$\Delta\varepsilon = \varepsilon_p \frac{t}{\delta}, \tag{3}$$

where, t is the thickness of the solvent layer and δ the thickness of the particle. Using this relation, we can estimate the value of the dielectric constant of the GO particles.

The ratio of the respective thickness of the GO layer and solvent layer can be estimated through the volume fraction ϕ_V, defined by the ratio of the volume of the particle and the total volume

$$\delta/t \sim \phi_V. \tag{4}$$

From this relation, by using the respective density of the solvents equal to 0.79 g ml^{-1} for 2-Propanol and 1.83 g ml^{-1} for GO we obtain a value of $\phi_V \sim 0.0291$ for a weight fraction of 6.5 wt%.

We deduce from this value that the dielectric constant of the particle is equal to ~1.0 for the dispersions in IPA. On the other hand, considering the volume fraction for Milli-Q water, equal to $\phi_V \sim 0.0361$ at a weight fraction of 6.5 wt%, we find a value of 2.3 for the dielectric constant of the GO particles in Milli-Q water.

Even if the two values found in Milli-Q water and IPA are just estimates of the dielectric constant of the particle, they are still significantly lower than the giant permittivity found in many other papers [7–15, 30].

It is also interesting to note a steep rise of the capacitance of the double layer with adding a small amount of GO. This increase is presumably due to the adsorption of ions at the surface of the electrodes.

Last, we also note that the dielectric properties of the sample does not show any dependence on the size of the flakes. This is expected as long as $t \gg \delta$. To confirm this expectation, we show in figure S7 the dielectric properties of a solution of small particles made by strong sonication. The results are in agreement with those found for larger particles. In particular C_{bulk} remains low, which reflects again the absence of giant permittivity of GO.

Conclusion

We have characterized the impedance of GO solutions at high concentrations in two different solvents. In both cases, we observed a large polarization of the electrodes. In order to determine the actual volumetric capacitance of the bulk and therefore the actual permittivity of the solutions, we use a very low constant cell and a simple equivalent circuit to model the electrical behavior of the system.

The good agreement between the model and the experiments allowed us to determine the permittivity of GO particles. We claim that the permittivity of GO is not particularly high. Typically, it has a relative permittivity varying from 1 to a few unites.

Therefore, we do not consider GO LCs as good candidates for high-k materials. Nevertheless, GO can be used as a suitable component for devices that exploit an interphase capacitance, like field effect transistors, as an electrolyte or as precursor for graphene based materials, but not as an additive to raise the permittivity of solvents and composites for electronics (capacitive sensing, energy storage and energy harvesting in variable capacitors).

Acknowledgments

The authors wish to thank the Cluster of Excellence AMADEus of Université de Bordeaux for the facilities and financial support.

ORCID iDs

M Alfonso https://orcid.org/0000-0002-5013-0861
A Colin https://orcid.org/0000-0001-8372-006X
P Poulin https://orcid.org/0000-0001-7748-8671

References

[1] Zhu Y W, Murali S, Cai W W, Li X S, Suk J W, Potts J R and Ruoff R S 2010 Graphene and graphene oxide: synthesis, properties, and applications *Adv. Mater.* **22** 3906–24
[2] Dreyer D R, Park S, Bielawski C W and Ruoff R S 2010 The chemistry of graphene oxide *Chem. Soc. Rev.* **39** 228–40
[3] Huang X, Qi X Y, Boey F and Zhang H 2012 Graphene-based composites *Chem. Soc. Rev.* **41** 666–86
[4] Kuilla T, Bhadra S, Yao D H, Kim N H, Bose S and Lee J H 2010 Recent advances in graphene based polymer composites *Prog. Polym. Sci.* **35** 1350–75
[5] Naficy S, Jalili R, Aboutalebi S H, Gorkin R A, Konstantinov K, Innis P C, Spinks G M, Poulin P and Wallace G G 2014 Graphene oxide dispersions: tuning rheology to enable fabrication *Mater. Horiz.* **1** 326–31
[6] Poulin P, Jalili R, Neri W, Nallet F, Divoux T, Colin A, Aboutalebi S H, Wallace G and Zakri C 2016 Superflexibility of graphene oxide *Proc. Natl Acad. Sci. USA* **113** 11088–93
[7] Liu J Z, Galpaya D, Notarianni M, Yan C and Motta N 2013 Graphene-based thin film supercapacitor with graphene oxide as dielectric spacer *Appl. Phys. Lett.* **103** 063108
[8] Hong X H, Yu W D, Wang A D and Chung D D L 2016 Graphite oxide paper as a polarizable electrical conductor in the through-thickness direction *Carbon* **109** 874–82
[9] Huang X Y, Zhi C Y, Jiang P K, Golberg D, Bando Y and Tanaka T 2012 Temperature-dependent electrical property transition of graphene oxide paper *Nanotechnology* **23** 455705
[10] Kumar K S, Pittala S, Sanyadanam S and Paik P 2015 A new single/few-layered graphene oxide with a high dielectric constant of 10^6: contribution of defects and functional groups *RSC Adv.* **5** 14768–79
[11] Hou Z L, Liu X D, Song W L, Fang H M and Bi S 2017 Graphene oxide foams: the simplest carbon-air prototypes for unique variable *Dielectr. J. Mater. Chem.* C **5** 3397–407
[12] Wan S, Bi H C, Zhou Y L, Xie X, Su S, Yin K B and Sun L T 2017 Graphene oxide as high-performance dielectric materials for capacitive pressure sensors *Carbon* **114** 209–16
[13] Wang D-W, Du A, Taran E, Lu G Q and Gentle I R 2012 A water-dielectric capacitor using hydrated graphene oxide film *J. Mater. Chem.* **22** 21085–91

[14] Gao W, Singh N, Song L, Liu Z, Reddy A L M, Ci L, Vajtai R, Zhang Q, Wei B and Ajayan P M 2011 Direct laser writing of micro-supercapacitors on hydrated graphite oxide films *Nat. Nanotechnol.* **6** 496–500
[15] Bayer T, Bishop S R, Perry N H, Sasaki K and Lyth S M 2016 Tunable mixed ionic/electronic conductivity and permittivity of graphene oxide paper for electrochemical energy conversion *ACS Appl. Mater. Interfaces* **8** 11466–75
[16] Mensah B, Kim S, Arepalli S and Nah C 2014 A study of graphene oxide-reinforced rubber nanocomposite *J. Appl. Polym. Sci.* **131** 40640
[17] Chen M H, Yin J H, Jin R, Yao L, Sua B and Lei Q Q 2015 Dielectric and mechanical properties and thermal stability of polyimide-graphene oxide composite films *Thin Solid Films* **584** 232–7
[18] Tantis I, Psarras G C and Tasis D 2012 Functionalized graphene—poly(vinyl alcohol) nnocomposites: physical and dielectric properties *Express Polym. Lett.* **6** 283–92
[19] Wang Y Q, Fang M J, Tian B B, Xiang P H, Zhong N, Lin H C, Luo C H, Peng H and Duan C G 2017 Transparent PVDF-TrFE/graphene oxide ultrathin films with enhanced energy harvesting performance *Chemistryselect* **2** 7951–5
[20] Sadasivuni K K, Ponnamma D, Kumar B, Strankowski M, Cardinaels R, Moldenaers P, Thomas S and Grohens Y 2014 Dielectric properties of modified graphene oxide filled polyurethane nanocomposites and its correlation with rheology *Compos. Sci. Technol.* **104** 18–25
[21] Kuwahara Y, Ueyama M, Yagi R, Koinuma M, Ogata T, Kim S, Matsumoto Y and Kurihara S 2013 Enhancement of alternating current electroluminescence properties by the addition of graphene oxide nanosheets as dielectric materials *Mater. Lett.* **108** 308–10
[22] Liu P J, Yao Z J and Zhou J T 2016 Mechanical, thermal and dielectric properties of graphene oxide/polyimide resin composite *High Perform. Polym.* **28** 1033–42
[23] Salomao F C, Lanzoni E M, Costa C A, Deneke C and Barros E B 2015 Determination of high-frequency dielectric constant and surface potential of graphene oxide and influence of humidity by kelvin probe force microscopy *Langmuir* **31** 11339–43
[24] Kavinkumar T, Sastikumar D and Manivannan S 2015 Effect of functional groups on dielectric, optical gas sensing properties of graphene oxide and reduced graphene oxide at room temperature *RSC Adv.* **5** 10816–25
[25] Yasin M, Tauqeer T, Zaidi S M H, San S E, Mahmood A, Kose M E, Canimkurbey B and Okutan M 2015 Synthesis and electrical characterization of graphene oxide films *Thin Solid Films* **590** 118–23
[26] Zhang Q, Scrafford F, Li M, Cao Z, Xia Z, Ajayan P M and Wei B 2014 Anomalous capacitive behaviors of graphene oxide based solid-state supercapacitors *Nano Lett.* **14** 1938–43
[27] Standley B, Mendez A, Schmidgall E and Bockrath M 2012 Graphene–graphite oxide field-effect transistors *Nano Lett.* **12** 1165–9
[28] Lee S K, Jang H Y, Jang S, Choi E, Hong B H, Lee J, Park S and Ahn J H 2012 All graphene-based thin film transistors on flexible plastic substrates *Nano Lett.* **12** 3472–6
[29] Eda G, Nathan A, Wobkenberg P, Colleaux F, Ghaffarzadeh K, Anthopoulos T D and Chhowalla M 2013 Graphene oxide gate dielectric for graphene-based monolithic field effect transistors *Appl. Phys. Lett.* **102** 133108
[30] Al-Zangana S, Iliut M, Boran G, Turner M, Vijayaraghavan A and Dierking I 2016 Dielectric spectroscopy of isotropic liquids and liquid crystal phases with dispersed graphene oxide *Sci. Rep.* **6** 31885
[31] Zamora-Ledezma C, Puech N, Zakri C, Grelet E, Moulton S E, Wallace G G, Gambhir S, Blanc C, Anglaret E and Poulin P 2012 Liquid crystallinity and dimensions of surfactant-stabilized sheets of reduced graphene oxide *J. Phys. Chem. Lett.* **3** 2425–30
[32] Yuan J, Luna A, Neri W, Zakri C, Schilling T, Colin A and Poulin P 2015 Graphene liquid crystal retarded percolation for new high-*k* materials *Nat. Commun.* **6** 8700
[33] Barsoukov E and Macdonald J R 2005 *Impedance Spectroscopy: Theory, Experiment, and Applications* 2nd edn (Hoboken, NJ: Wiley-Interscience)
[34] Mancinelli P, Fabiani D, Saccani A, Toselli M and Frechette M F 2015 Electrical AC and DC behavior of epoxy nanocomposites containing graphene oxide *J. Appl. Polym. Sci.* **132** 41923
[35] Cui L L, Lu X F, Chao D M, Liu H T, Li Y X and Wang C 2011 Graphene-based composite materials with high dielectric permittivity via an *in situ* reduction method *Phys. Status Solidi* A **208** 459–61
[36] Hong X H, Yu W D and Chung D D L 2017 Electric permittivity of reduced graphite oxide *Carbon* **111** 182–90
[37] Kuang B, Song W L, Ning M Q, Li J B, Zhao Z J, Guo D Y, Cao M S and Jin H B 2018 Chemical reduction dependent dielectric properties and dielectric loss mechanism of reduced graphene oxide *Carbon* **127** 209–17
[38] Toselli M, Fabiani D, Mancinelli P, Frechette M, Heid T, David E and Saccani A 2015 *In situ* thermal reduction of graphene oxide forming epoxy nanocomposites and their dielectric properties *Polym. Compos.* **36** 294–301
[39] Xing Y, Bai X and Zhang Y 2014 Mechanical, thermal conductive, and dielectric properties of fluoroelastomer/reduced graphene oxide composites *in situ* prepared by solvent thermal reduction *Polym. Compos.* **3** 1779–85
[40] Yousefi N, Sun X Y, Lin X Y, Shen X, Jia J J, Zhang B, Tang B Z, Chan M S and Kim J K 2014 Highly aligned graphene/polymer nanocomposites with excellent dielectric properties for high-performance electromagnetic interference shielding *Adv. Mater.* **26** 5480–7
[41] Hummers W S Jr and Offeman R E 1958 Preparation of graphitic oxide *J. Am. Chem. Soc.* **80** 1339
[42] Hu H, Quan H, Zhong B, Li Z, Huang Y, Wang X, Zhang M and Chen D 2018 A reduced graphene oxide quantum dot-based adsorbent for efficiently binding with organic pollutants *ACS Appl. Nano Mater.* **1** 6502–13
[43] Coleman B R, Knight T, Gies V, Jakubek Z J and Zou S 2017 Manipulation and quantification of graphene oxide flake size: photoluminescence and cytotoxicity *ACS Appl. Mater. Interfaces* **9** 28911–21
[44] Valles C, Young R J, Lomax D J and Kinloch I A 2014 The rheological behaviour of concentrated dispersions of graphene oxide *J. Mater. Sci.* **49** 6311–20
[45] Ben Ishai P, Talary M S, Caduff A, Levy E and Feldman Y 2013 Electrode polarization in dielectric measurements: a review *Meas. Sci. Technol.* **24** 102001
[46] Zakri C, Blanc C, Grelet E, Zamora-Ledezma C, Puech N, Anglaret E and Poulin P 2013 Liquid crystals of carbon nanotubes and graphene *Phil. Trans. R. Soc.* A **371** 20120499
[47] Kumar P, Maiti U N, Lee K E and Kim S O 2014 Rheological properties of graphene oxide liquid crystal *Carbon* **80** 453–61
[48] Kim J E, Han T H, Lee S H, Kim J Y, Ahn C W, Yun J M and Kim S O 2011 Graphene oxide liquid crystals *Angew. Chem.* **123** 3099–103
[49] Bard A J and Faulkner L R 2001 *Electrochemical Methods: Fundamentals and Applications* (New York: Wiley)
[50] Garcìa-Garcìa A, Vergaz R, Algorri J F, Geday M A and Otòn J M 2015 The peculiar electrical response of liquid crystal-carbon nanotube systems as seen by impedance spectroscopy *J. Phys. D: Appl. Phys.* **48** 375302
[51] Jung Lee H, Bai S-J and Seok Song Y 2017 Microfluidic electrochemical impedance spectroscopy of carbon composite nanofluids *Sci. Rep.* **7** 722
[52] Hubálek J 2015 Iterative precise conductivity measurements with IDEs *Sensors* **15** 12080–91

[53] Song J and Bazant M Z 2013 Effects of nanoparticle geometry and size distribution on diffusion impedance of battery electrodes *J. Electrochem. Soc.* **160** A15–24
[54] Yoon Y, Jo J, Kim S, Lee I G, Cho B J, Shin M and Hwang W S 2017 Impedance spectroscopy analysis and equivalent circuit modeling of graphene oxide solutions *Nanomaterials* **7** 446